

Lycopene Reduces Potassium Bromate-induced Structural Alterations in the Jejunal Mucosa of Adult Rats

Original
Article

Noha Gamal Bahey and Noha Ramadan Mohamed Elswaidy

Department of Histology and Cell Biology, Faculty of Medicine, Tanta University, Egypt

ABSTRACT

Introduction: Potassium bromate (KBrO_3) is an oxidizing agent that is widely used as a flour improver. However, it induces genotoxic and carcinogenic effects on different body organs in a dose and duration-dependent manner.

Aim of this Study: To explore the effects of KBrO_3 on the structure of the rat jejunal mucosa and investigate the potential role of lycopene, a strong antioxidant molecule, in preventing or ameliorating the effect of KBrO_3 .

Materials and Methods: Twenty-four adult male albino rats were used and divided equally into four experimental groups; control group, lycopene group that received 10mg of lycopene/kg/day/orally; KBrO_3 group that received 100mg of KBrO_3 /kg/day/orally and KBrO_3 and lycopene group that received KBrO_3 and lycopene in the same doses as in the previous groups. Animals were sacrificed after 4 weeks and the specimens from the jejunum were processed for histological, immunohistochemical, and ultrastructural examinations.

Results: The jejunal mucosa of the KBrO_3 treated group showed short and broad villi, discontinuity and desquamation of their lining epithelial cells, inflammatory cellular infiltration, and dilatation of the blood vessels. Moreover, there was a significant decrease in the number of goblet cells and PCNA immuno-stained nuclei in the jejunum. Ultramicroscopic examination showed swollen vacuolated mitochondria, dilated rough endoplasmic reticulum, and shrunken dark nuclei. Interestingly, the group treated with both lycopene and KBrO_3 showed less cytoplasmic vacuolation and mitochondrial abnormalities in the epithelial cells lining the villi. Furthermore, there was a significant improvement in the height of jejunal villi, the number of goblet cells, and PCNA immuno-stained nuclei.

Conclusion: KBrO_3 induced cellular damage in the rat jejunal mucosa which was prevented by coadministration of lycopene.

Received: 13 December 2020, **Accepted:** 31 December 2020

Key Words: Histopathology; jejunum; lycopene; PCNA; potassium bromate.

Corresponding Author: Noha Gamal Bahey, Department of Histology and Cell Biology, Faculty of Medicine, Tanta University, Egypt, **Tel.:** +447907942511, **E-mail:** nohabahey@gmail.com

ISSN: 1110-0559, Vol. 44, No.4

INTRODUCTION

Potassium bromate (KBrO_3) is a white crystal that is widely used as a food additive^[1]. It is the element of choice in bread making all over the world because of its low price, availability, and reliability in the production of different baked goods and cheese^[2].

Previous studies have reported the serious destructive effect of KBrO_3 on different organs such as the kidney^[3], liver^[4], thyroid gland^[5], and the central nervous system^[6]. Oxidative DNA damage was also reported as one of the serious effects of bromate^[7] and therefore it was considered as a potential carcinogen in both humans and animals^[8] and was banned from use in manufactured goods in several countries^[9].

Bromate is a strong oxidizer, and its administration increases protein oxidation, lipid peroxidation, and hydrogen peroxide levels. It also decreases the level of antioxidant agents indicating the induction of oxidative stress. These harmful effects occur in a dose-dependent manner as previously reported in experimental animals^[10].

Lycopene is an antioxidant which is found in high amounts in fruits and vegetables especially those with red or pink color, as well as in dietary supplements^[11]. The administration of lycopene has been shown to lessen the risk of different natural and chemical toxins^[11], decrease the severity of different chronic disorders such as cardiovascular diseases^[12], and reduce the inflammatory and carcinogenic activities^[13].

So, the aim of this work was to investigate the effect of KBrO_3 on the structure of the jejunum mucosa and to test the potential effect of lycopene as a strong antioxidant in preventing these structural changes.

MATERIAL AND METHODS

Chemicals

- Potassium Bromate (KBrO_3) is a white crystalline salt (Merk, 1.04912) that was dissolved in distilled water.
- Lycopene is a soft gel capsule (Swanson), each capsule contains 10mg of lycopene from natural tomato extract.

Animals and experimental design

Twenty-four Adult male albino rats were used in this study, with an average bodyweight of 200 grams. Rats were housed in clean properly ventilated cages with free access to water and a standard diet. Animals were allowed to habituate for one week in the animal house then were randomly divided into four equal groups (6 rats/group).

Group I (control group): rats did not receive any treatment.

Group II (Lycopene group): rats were given lycopene at a dose of 10 mg/kg/day, dissolved in 0.5ml of distilled water using a gastric tube for 4 weeks^[11,14].

Group III (Potassium bromate (KBrO₃) group): rats were given KBrO₃ at a dose of 100 mg/kg/day, dissolved in 0.5 ml of distilled water using a gastric tube for 4 weeks. KBrO₃ dose was calculated to reflect the amount normally utilized in the human diet^[4].

Group IV (KBrO₃ and lycopene group): rats were given both lycopene and KBrO₃ at the same doses and duration as in groups II and III, respectively).

All the procedures used in this study were carried out in accordance with the National Institutes of Health guide for the care and use of laboratory animals (NIH Publications No. 8023, revised 1978) and approved by the research ethics committee, Tanta University, Egypt.

Specimens processing and staining

At the end of the experiment, the rats were humanely culled by intraperitoneal injection of a terminal dose of pentobarbital at a dose of 50 mg/kg^[15]. Then a midline incision was made through the anterior abdominal wall and the jejunum was carefully dissected and flushed with normal saline to clean its interior. The jejunal samples were processed either for histological study using light microscope or for ultrastructure study using electron microscopes.

For the histological and immunohistochemical studies, the jejunal samples were fixed in 10% neutral buffered formalin for 24 hours and processed for paraffin embedding. Tissue sections were then either stained with hematoxylin and eosin (H & E) to study the general structure of jejunum^[16,17] or were stained with PAS (periodic acid Schiff) stain to highlight the goblet cells, in which the periodic acid oxidizes hydroxyl group within the carbohydrate with the formation of two free aldehyde groups. These free aldehydes react with Schiff reagent resulting in the bright red magenta color of glycogen and mucins^[18].

For immunohistochemistry, 5µm-thick jejunal sections were collected on coated slides and were deparaffinized, rehydrated, and exposed to heat mediated antigen retrieval with 0.1M sodium citrate buffer (pH 6.0) using a water bath at 85 for 30min. To prevent non-specific binding of the antibody, the sections were incubated for 1 hour at room

temperature with 5% normal goat serum in 0.3M phosphate buffer saline with triton-x 100. After that, the sections were incubated overnight at 4°C with (mouse monoclonal PCNA antibody (PC10), (ab29), Abcam, 1:1000). Then excess primary antibody was removed by washing the sections with PBS (3 times x5 minutes). Sections were then incubated with biotinylated secondary antibody (goat anti-mouse IgG H&L (HRP), ab205719, Abcam, 1:200) for two hours at room temperature. Avidin-biotin complex was added to the sections and the immunoreactivity was visualized using 3,3'-diaminobenzidine (DAB) as a chromogen. finally, the sections were counterstained with Mayer's hematoxylin, dehydrated and mounted with DPX^[19].

For transmission electron microscopic (TEM) examination, the jejunal samples were cut into small pieces 1mm³ and were fixed in 2.5% buffered glutaraldehyde in 0.1M phosphate buffer solution (pH 7.4) at 4°C for 2h. After that, the samples were washed with PBS (3x10 min) followed by post-fixation in 1% osmic tetroxide for (30 min). Then the samples were washed with PBS (3x10 min each) and were dehydrated by incubation in an ascending concentration of ethyl alcohol (30, 50, 70, 90, and 100%) and acetone for 30 min each. After dehydration, the samples were embedded in Araldite 502 epoxy resin and were cut using the Leica Ultracut UCT ultra-microtome and were stained with toluidine blue. After examination of the semi-thin sections (0.5 µm) in thickness, ultra-thin sections (70 nm) in thickness were cut, stained with uranyl acetate, and counterstained with lead citrate^[20]. The sections were examined and photographed using JEOL-JEM-100 SX electron microscope, Japan, at the electron microscope unit-Tanta University.

Morphometric analysis

The light microscopic images were analyzed using ImageJ software and the following parameters were measured from non-overlapping random fields (3 random fields/section, and 3 sections/rat):

1. The total mucosal thickness was measured from the apex of the villus to the muscularis mucosae using H&E-stained sections at 100X magnification.
2. The villus height was measured from the apex of the villus to the villus-crypt junction using H&E-stained sections at 100X magnification.
3. The crypt depth was measured from the villus-crypt junction to the end of the crypt using H&E-stained sections at 100X magnification.
4. The number of goblet cells in both villi and crypts was measured from PAS-stained sections at 200X magnification.
5. The number of PCNA positive nuclei per crypt was measured from PCNA immuno-stained jejunal sections at 400X magnification.

Statistical analysis

Comparison between the experimental groups was carried out using Graph Pad Prism 8.0 software, using one-way (ANOVA) with Tukey's post-hoc test. All the values were expressed as the mean value \pm standard error of the mean (Mean \pm SEM). Differences were regarded as significant if probability value (p) is <0.05 .

RESULTS

Light microscopic study

Hematoxylin & eosin staining sections showed normal histological structure and well-preserved cellular integrity of the rat jejunum in the control and lycopene-treated groups. The jejunum showed four main layers: mucosa, submucosa, muscularis externa, and serosa. The jejunal mucosa characterized by multiple villi and crypts. The villi are finger-like projections with a core of loose connective tissue, while crypts are invaginations in the lamina propria forming simple tubular glands (crypts of Lieberkühn). The villi are covered by tall columnar epithelial cells with basal oval nuclei and acidophilic cytoplasm as well as goblet cells that appeared as clear empty spaces in-between epithelial cells (Figure 1).

This normal jejunal structure was altered in KBrO₃ treated group where several histopathological changes and evidence of cellular degeneration were observed. Most of the villi were short and broad, while others were fused with areas of discontinuity, destruction, and desquamation of their lining epithelial cells which are characterized by pyknotic nuclei and cytoplasmic vacuolation (Figure 2). Moreover, there was a no table destruction and loss of normal structure of some crypts with cytoplasmic vacuolation in their lining epithelial cells (Figure 3). There were also dilated and congested blood vessels in the submucosa with focal areas of inflammatory cellular infiltration in the lamina propria of the villi and in-between the crypts that extended into the submucosa and muscularis externa (Figures 2,3).

On the other hand, coadministration of lycopene with KBrO₃ reduced the cellular changes observed in the jejunum of the group treated with KBrO₃ alone and showed well-oriented villi lined with intact columnar epithelial cells and goblet cells. However, few villi showed areas of epithelial discontinuity in addition to the presence of pyknotic nuclei and cytoplasmic vacuolation in few epithelial cells (Figure 4).

Quantitative analysis of the light microscopic images displayed that there was a significant decrease in the total mucosal thickness ($p<0.0001$) and the mean villus height ($p<0.0001$) in KBrO₃ treated groups compared to both the control and the lycopene treated groups. On the other hand, co-administration of the lycopene with KBrO₃ induced a significant increase in the total mucosal thickness ($p<0.0001$), and the mean villus height ($p<0.0001$) in comparison to KBrO₃ treated group. There was no significant difference between the lycopene and

KBrO₃ treated group when compared to the control and the lycopene groups. However, analysis of the mean crypt depths did not show any significant difference between the experimental groups (Figure 5).

PAS staining of the jejunal mucosa showed numerous magenta/red-stained goblet cells in the lining epithelial cells of both villi and crypts in both the control and lycopene treated groups. On the other hand, there was a significant reduction ($p<0.001$) in the mean number of PAS-stained cells in both villi and crypts in KBrO₃- treated group. Interestingly, there was a significant increase ($p<0.001$) in the number of PAS-stained cells in the group received both KBrO₃ and lycopene compared to KBrO₃ treated group (Figure 6).

PCNA immunohistochemical staining of jejunal mucosa showed a strong nuclear immunoreaction and a numerous PCNA stained nuclei in the control and lycopene treated groups. While KBrO₃ treated group showed a weak PCNA immunostaining as well as a significant decrease ($p<0.0001$) in the mean numbers of PCNA positive nuclei in most of the crypt's cells compared to the control and the lycopene treated group. On the other hand, the KBrO₃ and the lycopene treated group showed a moderate PCNA immunostaining and a significant increase ($p<0.001$) in the mean number of PCNA stained nuclei compared to KBrO₃ treated group (Figure 7).

Transmission electron microscopic study

The Ultrathin sections of jejunal mucosa of the control and the lycopene treated groups showed similar morphology. The lining epithelial cells of the mucosa revealed regularly arranged closely packed enterocytes with single, basal, oval euchromatic nuclei surrounded by multiple rough endoplasmic reticula and abundant mitochondria. The luminal surface of the enterocytes had apical continuous regular microvillus border with extensive interdigitations between the lateral cell membrane of adjacent cells (Figure 8).

Ultrathin sections of the jejunal mucosa of the KBrO₃ treated group showed vacuolation and rarefaction of the cytoplasm of enterocytes and numerous mitochondria with disrupted cristae in the cytoplasm of enterocytes (Figure 9). Some enterocytes showed shrunken dark nuclei, loss of the upper part of the enterocyte, and detached microvilli (Figure 10). While, other enterocytes showed swollen vacuolated mitochondria, and irregularly shaped fragmented nucleus (Figure 11). Moreover, the enterocytes presented with dilatation in RER cisternae, corrugation, and discontinuity of their nuclear membrane along with short sparse microvilli. There were also wide intercellular spaces in between adjacent enterocytes with focal loss of microvillus border of some enterocytes (Figure 12). The lamina propria of the jejunal mucosa showed infiltration with multiple inflammatory cells such as plasma cells, mast cells, and an acidophil (Figure 13).

Alternatively, the ultrathin sections of the jejunal mucosa of KBrO_3 and lycopene treated group showed apparently normal closely packed enterocytes with regular

continuous microvillus border. However, cytoplasmic vacuolation and mitochondria with disrupted cristae were still observed in few enterocytes (Figure 14).

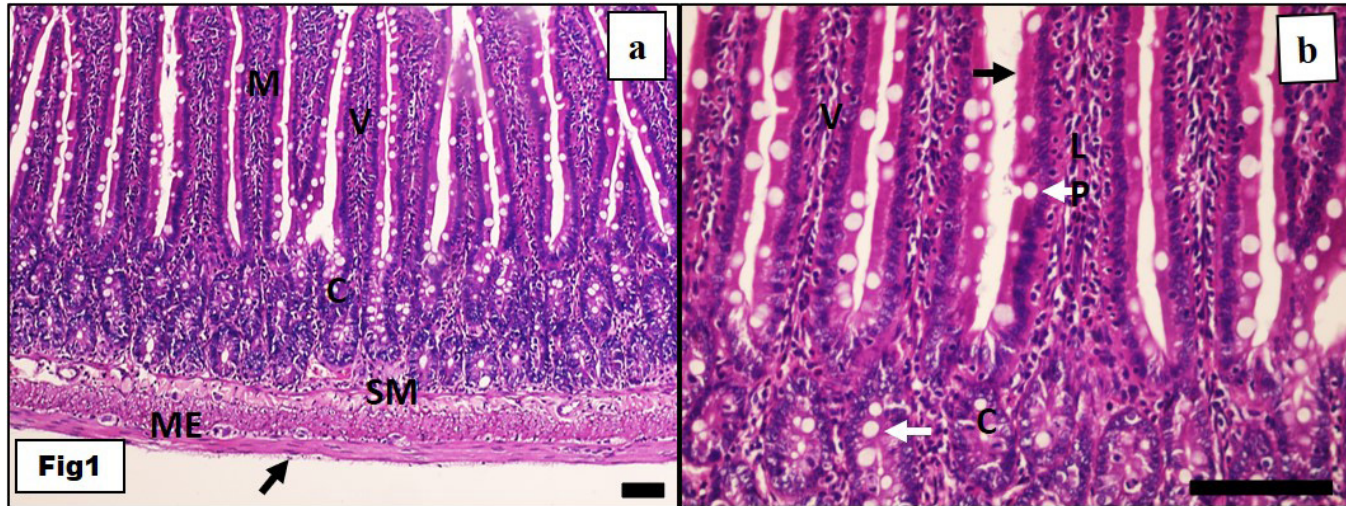


Fig. 1: Photomicrographs of rat jejunum from the control group showing (a) mucosa (M), submucosa (SM), musculosa externa (ME) and serosa (arrow). (b) Higher magnification of (a) showing mucosa with finger-like villi (V) with a core of lamina propria (LP) and simple tubular crypts (C) opening at the base of the villi. The villi are covered with simple columnar cells with basal oval nuclei and apical brush border (black arrow) that intermingles with goblet cells (white arrow). (H.&E., scale bar=50 μm).

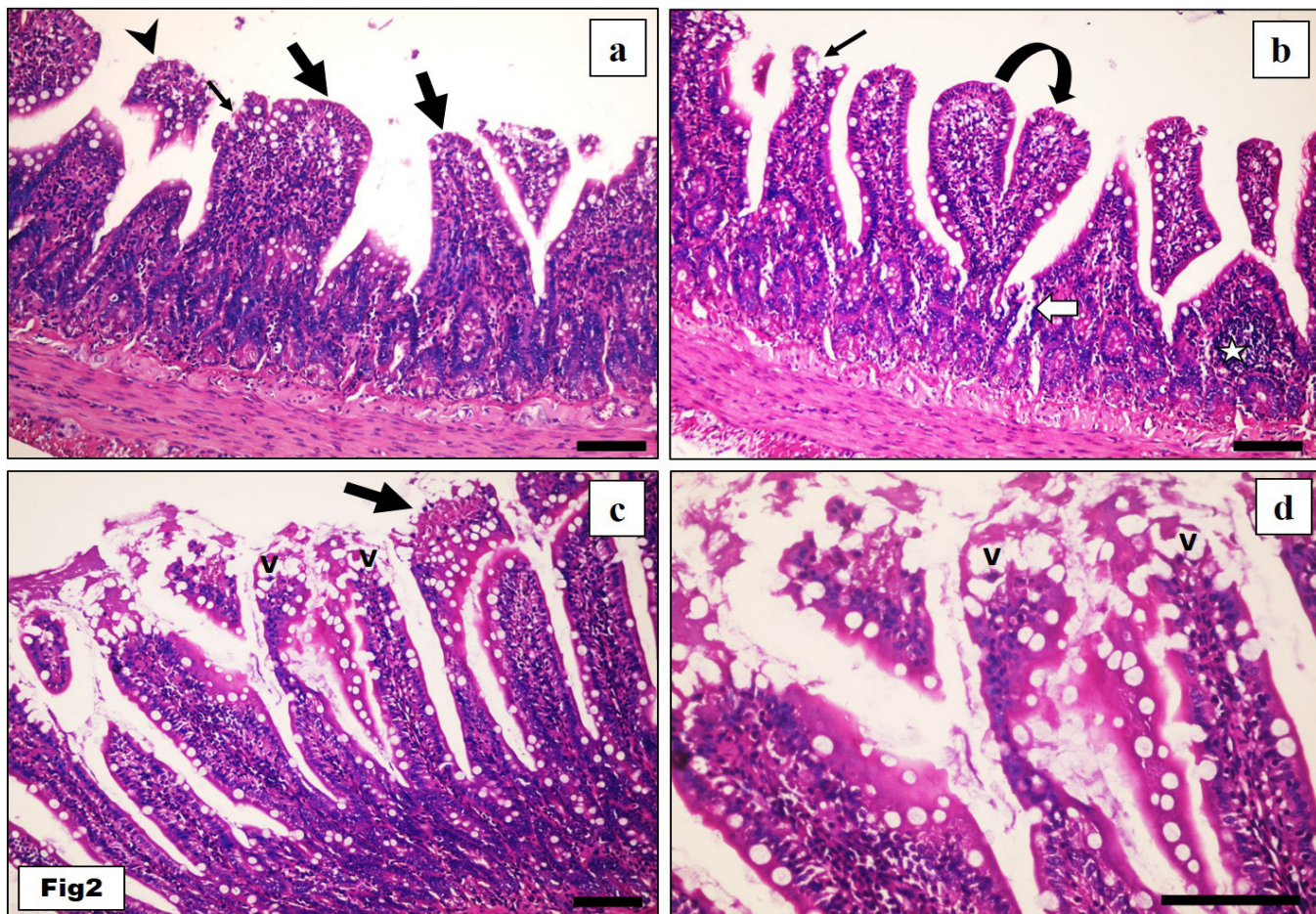


Fig. 2: Photomicrographs of rat jejunum from the KBrO_3 treated group showing (a) short and broad intestinal villi (thick arrow) with discontinuity (thin arrow) and desquamation (arrowhead) in the lining epithelial cells. (b) villus fusion (curved arrow) and discontinuity (thin arrow) of the villus lining epithelial cells. Some crypts showed destruction of their lining epithelial cells (white arrow) with focal area of mononuclear cellular infiltration (star). (c) some villi showed areas of sloughing of their lining epithelial cells (arrow) that mostly had cytoplasmic vacuolation (v) (d) higher magnification of (c). (H.&E.; Scale bar = 50 μm).

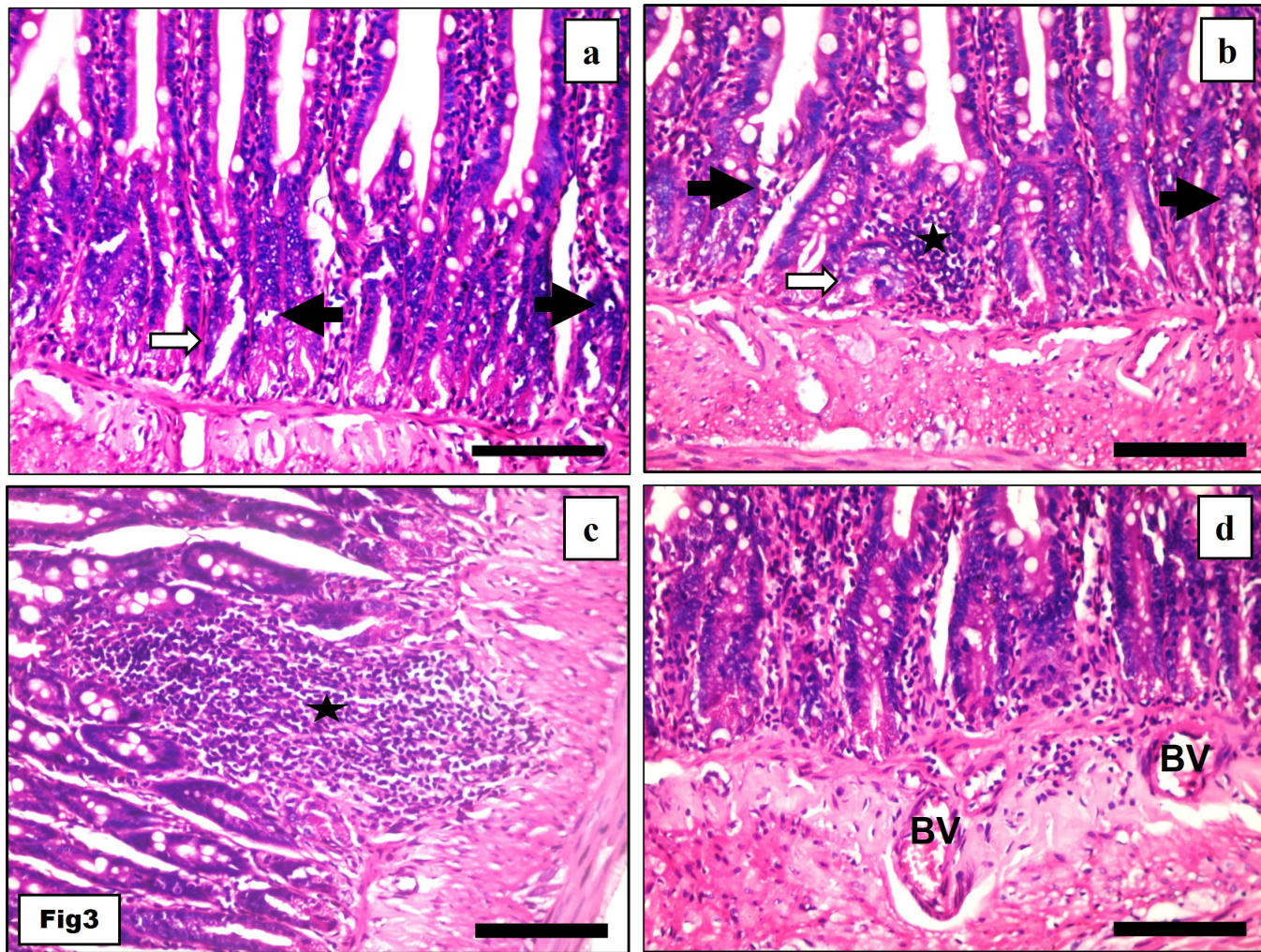


Fig. 3: Photomicrographs of rat jejunum from KBrO₃ treated group showing (a-b) destruction and loss of normal structure of some crypts (white arrow), cytoplasmic vacuolation with deeply stained pyknotic nuclei of some epithelial cells lining the crypt (black arrow), focal area of mononuclear cellular infiltration between the crypts (star). (c) large area of mononuclear cellular infiltration (star) between the crypt that extended into the submucosa and musculosa externa with (d) dilatation and congestion of the blood vessels (BV). (H.& E.; Scale bar = 50µm).

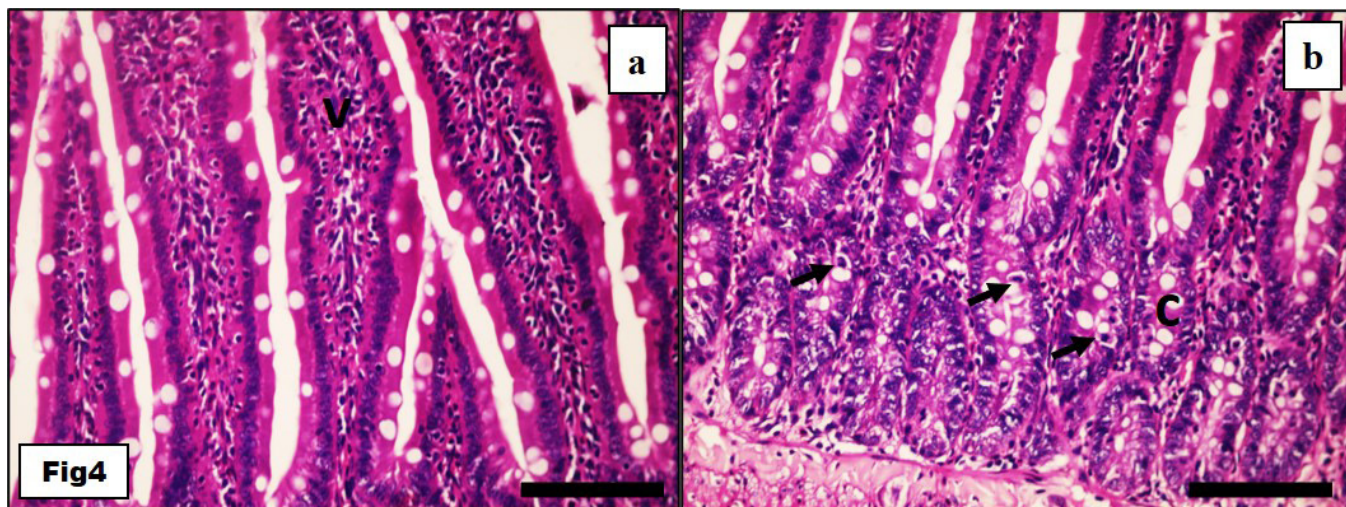


Fig. 4: Photomicrographs of rat jejunum from the KBrO₃ and lycopene treated group showing (a) well oriented villi (v) that preserved the normal structure. (b) intestinal crypts (c) with some vacuolated cells with pyknotic nuclei (arrow) are noted in their lining epithelial cells. (H.& E.; Scale bar = 50µm).

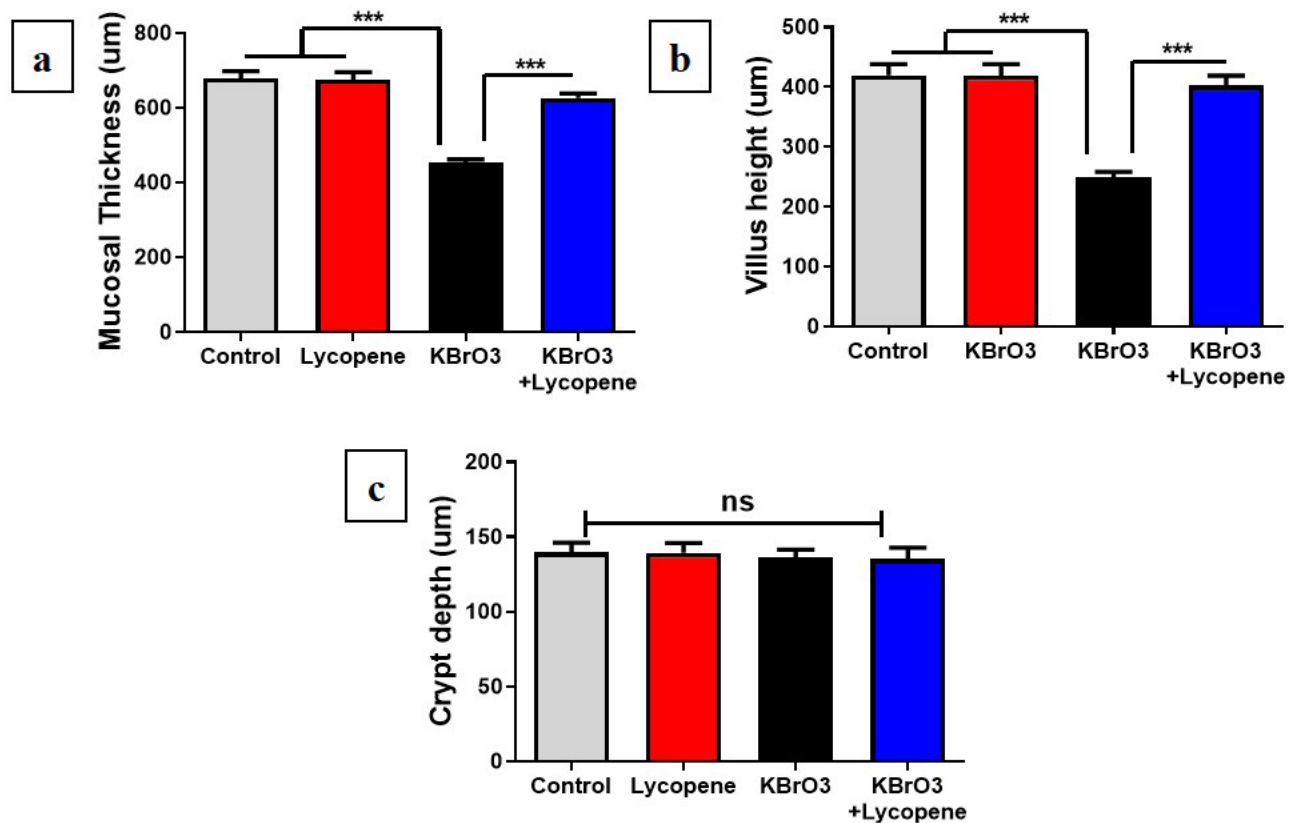


Fig. 5: Quantitative analysis of (a) total mucosal thickness, (b) villus height, and (c) crypt depth in the jejunal mucosa of the control, lycopene, KBrO₃ and the combined KBrO₃ and lycopene treated groups. Data are presented as mean \pm SEM, ** P <0.001, *** P <0.0001, ns: nonsignificant.

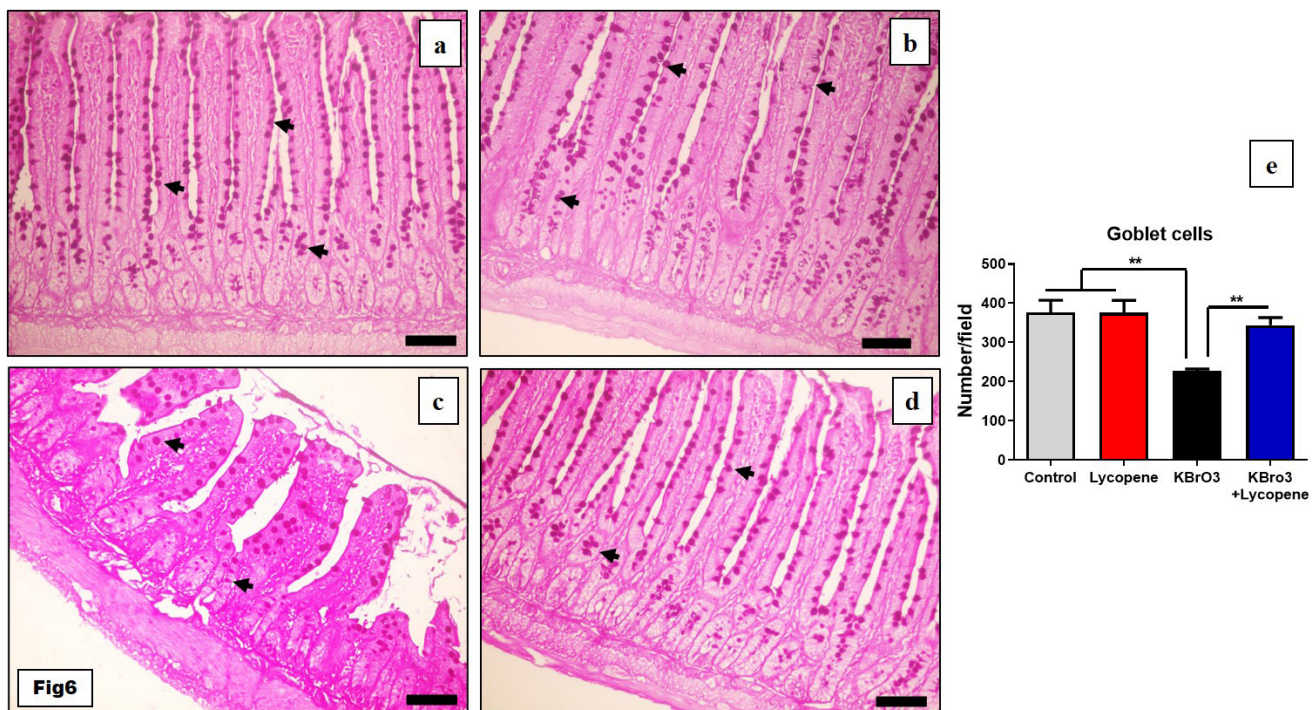


Fig. 6: photomicrographs of PAS stained jejunal sections displayed numerous magenta red stained goblet cells (arrow) in the lining epithelial cells of both villi and crypts of (a) control and (b) lycopene treated groups. (c) KBrO₃ treated group showing a significant reduction in the number of PAS-stained cells, that significantly increased in (d) the lycopene and KBrO₃ treated group. (PAS, scale bar=50 µm). (e) the mean number of the goblet cells per field in all the experimental groups. Data are presented as mean \pm SEM, ** P <0.001.

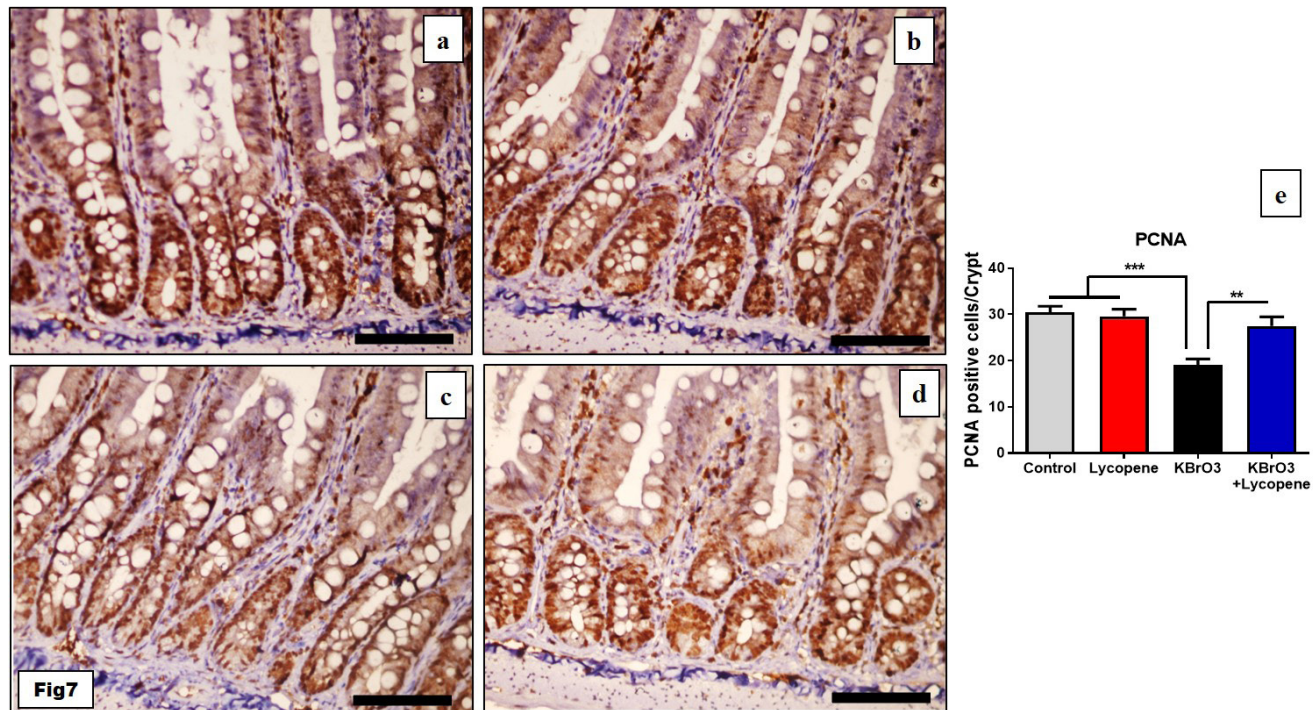


Fig. 7: photomicrographs of PCNA immunohistochemical staining of jejunum showing a strong positive nuclear immunoreaction (brown) in the lining epithelial of (a) control group and (b) lycopene treated group. (c) KBrO₃ treated group showing a weak PCNA positive nuclear immunoreaction. (d) lycopene and KBrO₃ treated group showing a moderate PCNA positive nuclear immunoreaction in lining epithelial cells (PCNA immunostaining, scale bar= 50µm). (e) the mean number of PCNA positive nuclei per crypt in the jejunal mucosa of all the experimental groups. Data are presented as mean ±SEM, ***P*<0.001, ****P*<0.0001.

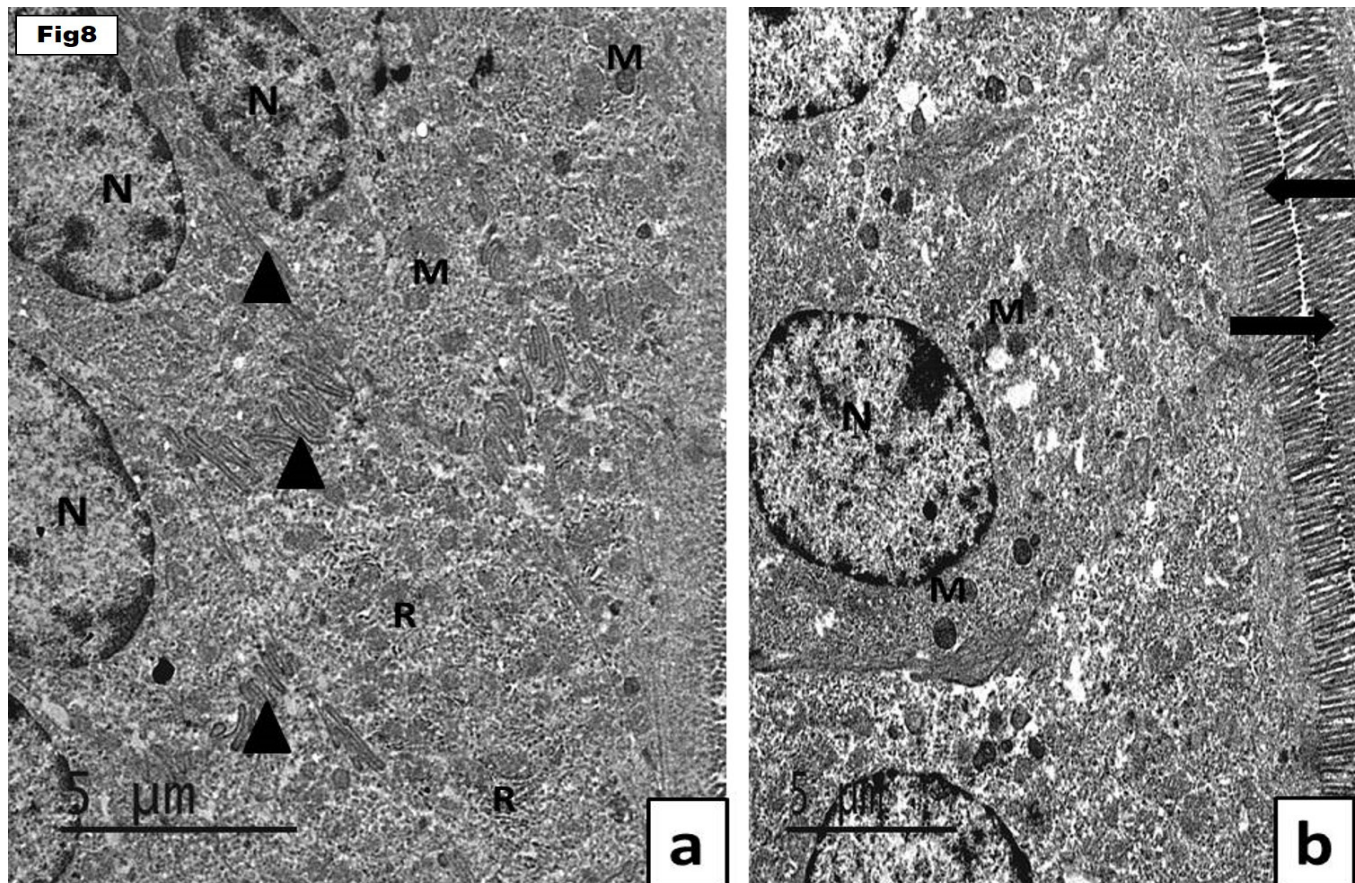


Fig. 8 (a and b): Electron micrographs of rat jejunum from the control group showing (a) regularly arranged closely packed enterocytes with basal oval euchromatic nuclei (N) and prominent nucleoli. The cytoplasm showed multiple mitochondria (M), RER (R), extensive interdigitations of the lateral cell membranes of adjacent cells (head arrow). (b) the enterocytes have regular continuous microvillous border (arrow). (scale bar= 5 µm).

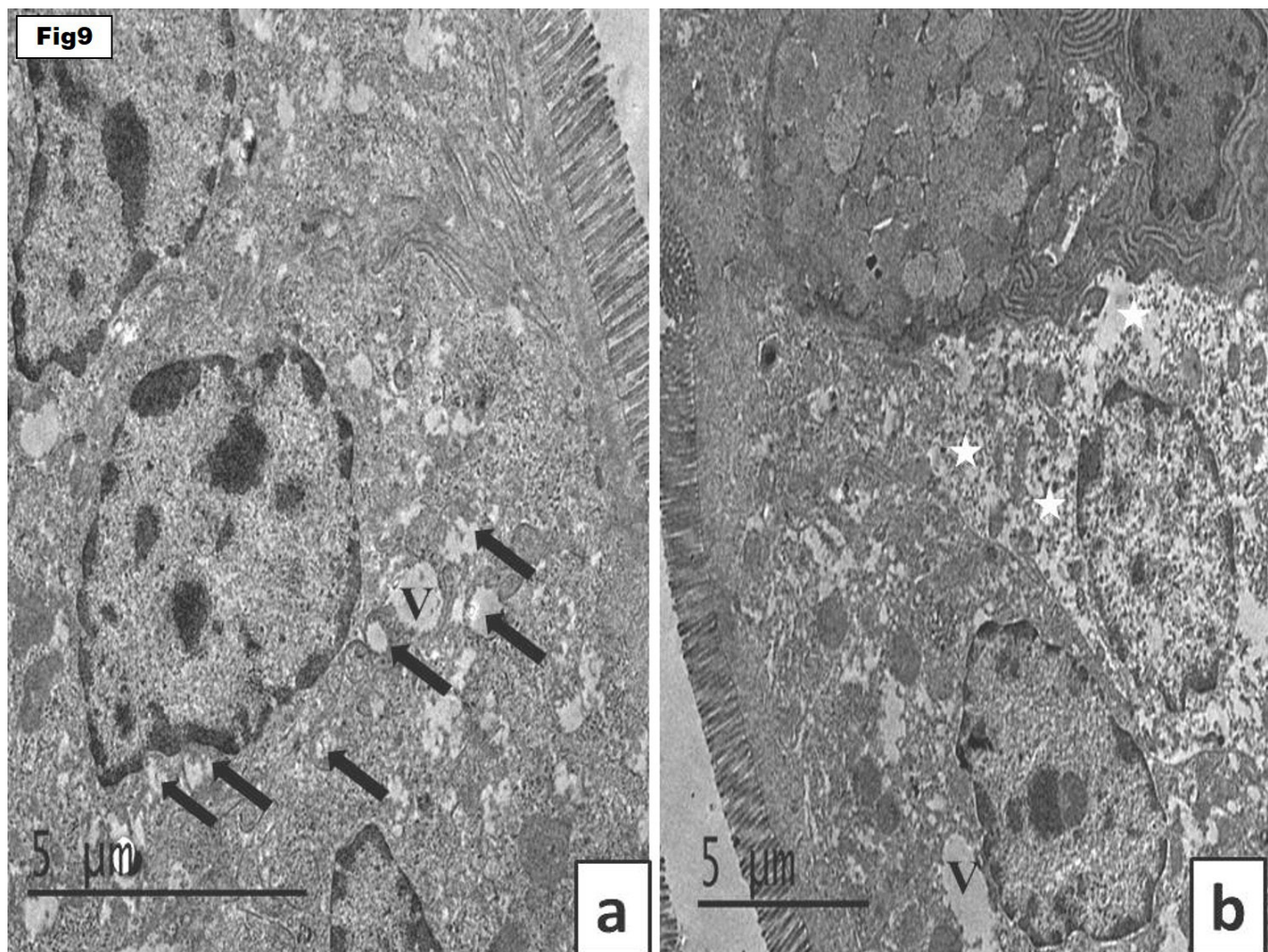


Fig. 9 (a and b): Electron micrographs of rat jejunum from KBrO_3 treated group showing (a) enterocytes with cytoplasmic vacuolation (V) and multiple mitochondria of disrupted cristae (arrow). (b) the enterocyte presented with areas of cytoplasmic rarefaction (star) around the nucleus. (scale bar= 5 μm).

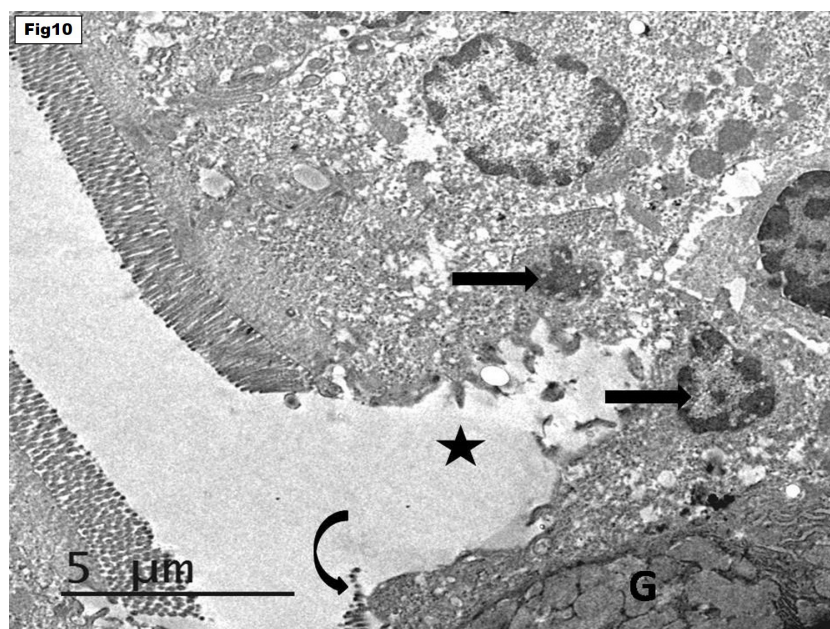


Fig. 10: Electron micrograph of rat jejunum from KBrO_3 treated group showing enterocyte with shrunken dark nuclei (arrow), loss of the upper part of the enterocyte (star) with detached microvilli (curved arrow). Notice the presence of goblet cell (g). (scale bar= 5 μm).

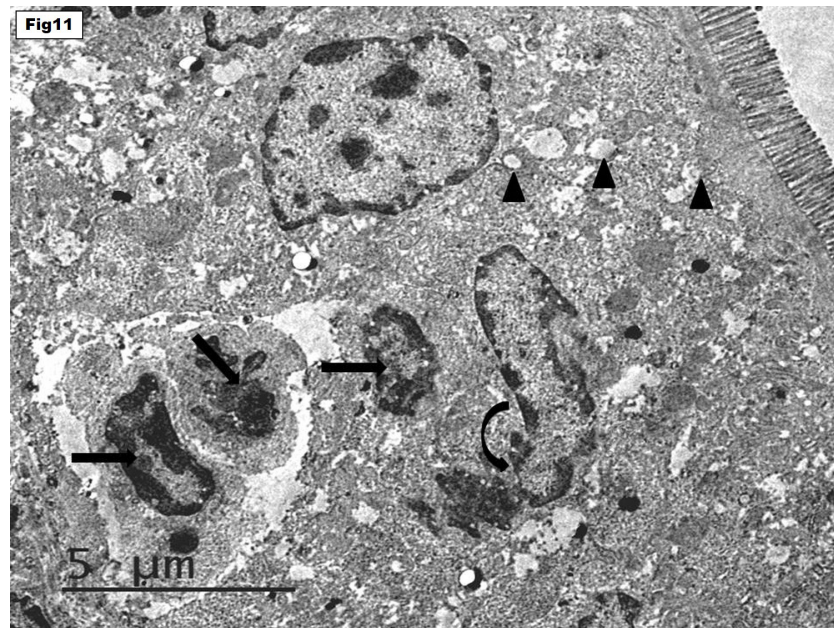


Fig. 11: Electron micrograph of rat jejunum from KBrO₃ treated group showing enterocytes presented with swollen vacuolated mitochondria (arrowhead), shrunken nuclei (arrow) and irregularly shaped fragmented nucleus (curved arrow). (scale bar= 5 μ m).

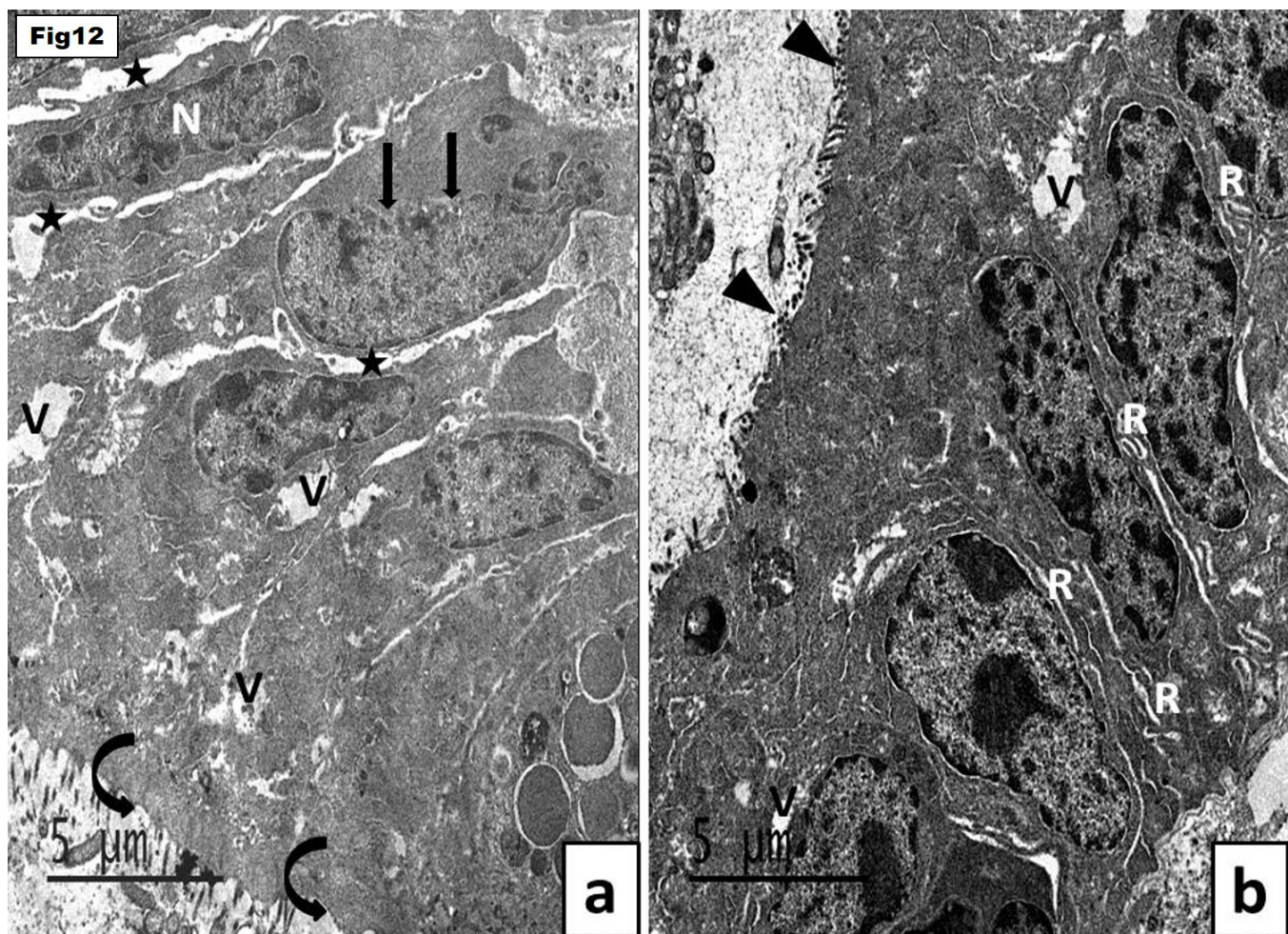


Fig. 12 (a and b): Electron micrographs of rat jejunum from KBrO₃ treated group showing (a) enterocytes with multiple cytoplasmic vacuolation (V), some nuclei presented with corrugation of their nuclear membrane (N) while others displayed discontinuity of their nuclear membrane (arrow). There are wide intercellular spaces between enterocytes (star) with focal loss of microvillus border (curved arrow). (b) the enterocytes also showing short sparse microvilli (arrowhead) with dilated RER cisternae (R). (scale bar= 5 μ m).

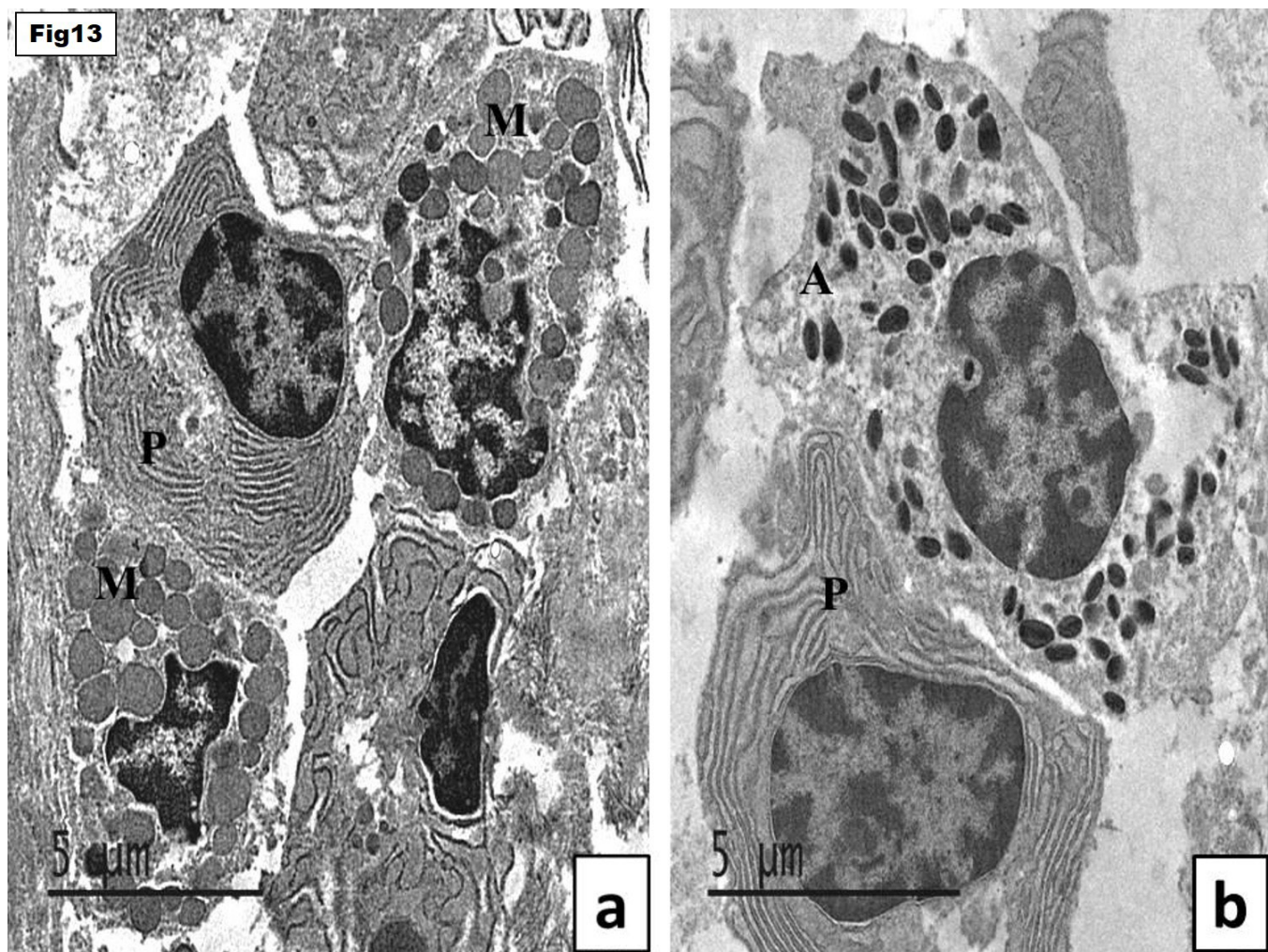


Fig. 13 (a and b): Electron micrographs of rat jejunum from KBrO_3 treated group showing infiltration of the lamina propria with mononuclear inflammatory cells as plasma cells (P), mast cells (M) and an acidophil (A). (scale bar= 5 μm).

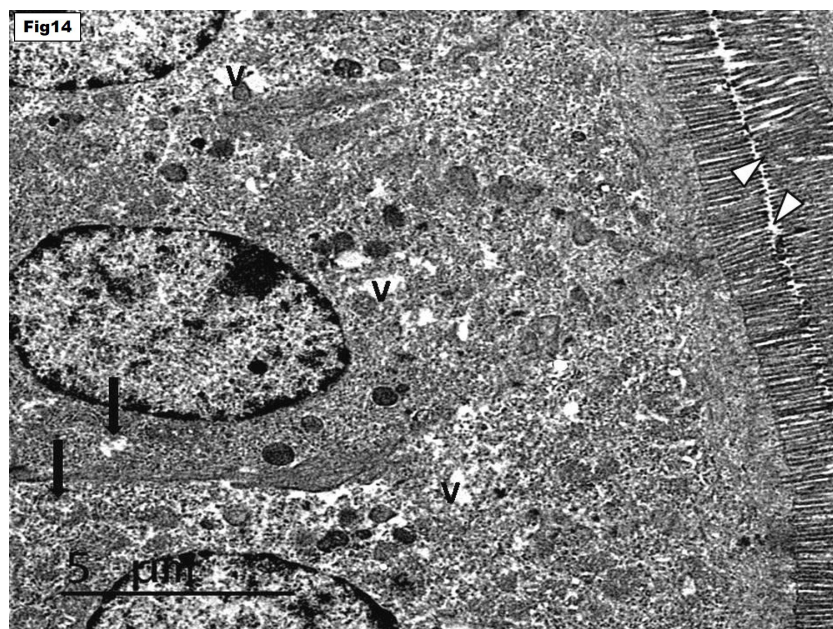


Fig. 14: Electron micrograph of rat jejunum from KBrO_3 and lycopene treated group showing apparently normal closely packed enterocytes with minimal cytoplasmic vacuolation, few numbers of mitochondria with disrupted cristae and regular continuous microvillus border (arrowhead). (scale bar= 5 μm).

DISCUSSION

Potassium bromate is a food additive that is widely used as a maturing agent for flour. It is also extensively used in the production of cheese, fish paste, cold wave hair solutions, and a variety of cosmetic and pharmaceutical products^[2]. However, previous studies have shown the damaging effect of KBrO₃ on different organs such as kidney and liver^[21,22].

In this study, the jejunum of KBrO₃-treated rats showed discontinuity in the epithelial cells lining the villi, marked destruction, and sloughing off some epithelial and goblet cells of intestinal villi with a significant decrease in the villus height and total mucosal thickness. As well as the presence of mononuclear cellular infiltration and dilated blood vessels. Similar results were reported previously in the duodenal mucosa of KBrO₃ treated rats, in the form of loss and disorganization of the surface enterocytes, loss of brush border, and infiltration with inflammatory^[23].

The harmful effect of KBrO₃ may mainly belong to the imbalance between the antioxidants and the excess generation of the free radicals. The free radicals react with lipids, proteins, and nucleic acids leading to tissue damage^[24,25]. They also induce a disruptive effect on the microcirculation in the intestinal mucosa with subsequent desquamation of the epithelial cells^[26]. The toxic effect of KBrO₃ on the rat intestine also reduces the tissue content of glutathione which is a crucial antioxidant molecule^[27,28].

The loss of intestinal cell with KBrO₃ could also be clarified by its role in enhancing the activity of the acid phosphatase with subsequent lysosomal cell death^[23,29]. Moreover, KBrO₃ stimulates the reduction in the alkaline phosphate enzyme (ALP) activity in the intestine. Which could affect the transport of required ions and nutrients across the cell membrane with subsequent cell starvation and death^[30].

Another possible mechanism for the damaging effect of KBrO₃ is the induction of the immune complex^[31]. That supported by the presence of mononuclear cellular infiltration in the villi and in-between the crypts. This cellular infiltration could also be a consequences of the generation of reactive oxygen species that can activate the transcription factors and stimulate the secretion of pro-inflammatory cytokines such as TNF- α and IL-6^[32].

KBrO₃ treated group also showed a weak positive nuclear immunoreaction for PCNA in many crypt cells, which indicates a reduction in cell division in the intestinal crypts. This alteration could be a result of chromosomal aberrations induced by KBrO₃. Similar findings were previously reported in human peripheral lymphocytes cell culture that displayed a reduction in the mitotic index (MI) and the cell proliferation index following the treatment with KBrO₃^[33]. However, another study reported a time-and dose-dependent increase in area fraction of PCNA immunostaining in the tongue epithelial, connective, and muscle cells in rats treated with KBrO₃^[34].

The mean number of goblet cells was found to be significantly low in KBrO₃ treated group compared to the control group. Which may be due to massive intestinal mucosal damage caused by KBrO₃-induced oxidative stress. Different cytoplasmic alterations were also observed the lining epithelial cells of jejunal mucosa induced by KBrO₃ administration. Mitochondrial swelling is one of the main ultrastructure variations that observed in this study and could be an early sign of cell damage where the vacuoles start within the mitochondria then extend through the cristae causing their distortion^[35].

The tissue oxidative stress in the main cause of mitochondrial damage which encourages the formation of a channel called mitochondrial permeability transition pore. Opening this channel induces loss of mitochondrial membrane potential, depletion of ATP, reduction in protein synthesis and accumulation of intracellular calcium. The increase in cytosolic calcium has a harmful effect on the cells through activation of caspases with subsequent cellular apoptosis. As well as through activation of protease enzymes with subsequent break down of membrane and cytoskeletal proteins which resulted in detachment and focal loss of microvilli^[36,37].

The widening of the intercellular space between enterocytes was also observed in KBrO₃ treated group. That could be due to the defect in sodium-potassium-ATPase activity induced by KBrO₃, resulting in reducing the absorptive function of enterocytes with accumulation of nutrients and fluid^[38]. The cellular degeneration in the jejunal lining epithelial cells was also detected with KBrO₃ administration which could belong to the reduction of cellular energy production and protein synthesis with subsequent degeneration^[39,40].

On the other hand, the concomitant administration of lycopene with KBrO₃ showed a clear improvement in the structure of the rat jejunum. As well as a significant increase in the total mucosal thickness, the height of villi, the mean number of goblet cells and PCNA immune-stained nuclei compared to the KBrO₃ treated group. Similar results were reported in the previous study that revealed the significant role of lycopene in improving the intestinal alterations induced by methotrexate in experimental rats due to the decrease of oxidative stress and pro-inflammatory cytokines^[14].

Lycopene is one of the most powerful antioxidants and anti-inflammatory agents among all the dietary carotenoids, which protect the mammalian cells from oxidation through binding to the free oxygen radicals such as hydrogen peroxide, nitrogen dioxide, and hydroxyl radicals^[41,42]. That was confirmed by using lycopene as a treatment in different chronic gastrointestinal diseases such as peptic ulcer, gastric cancer, and gastroesophageal reflux^[43].

CONCLUSION

KBrO₃ induced histological and ultrastructural alterations in the jejunal mucosa of adult male albino rat,

that can be prevented by concomitant administration of lycopene through its antioxidant properties.

CONFLICT OF INTERESTS

There are no conflicts of interest.

REFERENCES

1. Shanmugavel V, Komala Santhi K, Kurup AH, Kalakandan S, Anandharaj A, Rawson A: Potassium bromate: Effects on bread components, health, environment and method of analysis: A review. *Food Chem* 2020, 1(311):125964.
2. Oloyede OB, Sunmonu TO: Potassium bromate content of selected bread samples in Ilorin, Central Nigeria and its effect on some enzymes of rat liver and kidney. *Food Chem Toxicol* 2009, 47(8):2067-2070.
3. Ali BH, Za'abi MA, Karaca T, Suleimani YA, Balushi KAA, Manoj P, Ashique M, Nemmar A: Potassium bromate-induced kidney damage in rats and the effect of gum acacia thereon. *Am J Transl Res* 2018, 10(1):126-137.
4. Altoom NG, Ajarem J, Allam AA, Maooda SN, Abdel-Maksoud MA: Deleterious effects of potassium bromate administration on renal and hepatic tissues of Swiss mice. *Saudi J Biol Sci* 2018, 25(2):278-284.
5. Stasiak M, Lewiński A, Karbownik-Lewińska M: (Relationship between toxic effects of potassium bromate and endocrine glands). *Endokrynol Pol* 2009, 60(1):40-50.
6. Allam AA, Othman SI, Mahmoud AM: Deleterious effects of perinatal exposure to potassium bromate on the development of offspring of Swiss mice. *Toxicol Ind Health* 2019, 35(1):63-78.
7. Ahmad MK, Khan AA, Ali SN, Mahmood R: Chemoprotective effect of taurine on potassium bromate-induced DNA damage, DNA-protein cross-linking and oxidative stress in rat intestine. *PLoS One* 2015, 10(3):e0119137.
8. Chauhan D, Jain P: A scientific study of genotoxic-carcinogenic impacts of Potassium Bromate as food additive on human health. *International Research Journal of Engineering and Technology* 2016, 3(6):1136-1139.
9. Achukwu PU, Ufelle SA, Ukaejiofo EO, Ejezie FE, Nwachukwu DN, Nwagha UI, Nworie WC, Anyachie USB: The effect of potassium bromate on some haematological parameters of wistar rats. *Nigerian journal of physiological sciences* 2009, 24(1):59-61.
10. Ahmad MK, Mahmood R: Oral administration of potassium bromate, a major water disinfection by-product, induces oxidative stress and impairs the antioxidant power of rat blood. *Chemosphere* 2012, 87(7):750-756.
11. Hedayati N, Naeini MB, Nezami A, Hosseinzadeh H, Wallace Hayes A, Hosseini S, Imenshahidi M, Karimi G: Protective effect of lycopene against chemical and natural toxins: A review. *Biofactors* 2019, 45(1):5-23.
12. Wang X, Lv H, Gu Y, Wang X, Cao H, Tang Y, Chen H, Huang C: Protective effect of lycopene on cardiac function and myocardial fibrosis after acute myocardial infarction in rats via the modulation of p38 and MMP-9. *J Mol Histol* 2014, 45(1):113-120.
13. Jiang LN, Liu YB, Li BH: Lycopene exerts anti-inflammatory effect to inhibit prostate cancer progression. *Asian J Androl* 2018, 21(1):80-85.
14. Yucel Y, Tabur S, Gozeneli O, Kocarslan S, Seker A, Buyukaslan H, Savik E, Aktumen A, Ozgonul A, Uzunkoy A *et al*: The effects of lycopene on intestinal injury due to methotrexate in rats. *Redox Rep* 2016, 21(3):113-118.
15. Gaertner DJ, Hallman TM, Hankenson FC, Batcherder MA: Anesthesia and analgesia for laboratory rodents. In: *Anesthesia and analgesia in laboratory animals*. 2nd edn. San Diego, CA. Boston.: Academic press,; 2008: 239 -240.
16. Bancroft M, Gamble JD. In: *Theory and Practice of Histological Techniques*. 6th edn. London: Churchill Livingstone; 2008: 121-122.
17. Chandler DE, Roberson RW: Preparation of specimens for light and electron microscopy In: *Bioimaging, Current Concepts in Light and Electron Microscopy*. LIC. Canda. UK: Jones and Bartlett Publishers, LIC; 2008: 29-58.
18. Kiernan JA: Histological and histochemical methods. In: *theory and practice*. 3rd edn. Oxford: Butterworth-Heinemann; 1999: 320–390.
19. Ramos-Vara JA, Kiupel M, Baszler T, Bliven L, Brodersen B, Chelack B, Czub S, Del Piero F, Dial S, Ehrhart EJ *et al*: Suggested guidelines for immunohistochemical techniques in veterinary diagnostic laboratories. *J Vet Diagn Invest* 2008, 20(4):393-413.
20. Suvarna KS, Layton C, Bancroft JD: *Bancroft's Theory and Practice of Histological Techniques*, 8th edn. China: Elsevier; 2019.
21. Farombi EO, Alabi MC, Akuru TO: Kolaviron modulates cellular redox status and impairment of membrane protein activities induced by potassium bromate (KBrO₃) in rats. *Pharmacol Res* 2002, 45(1):63-68.
22. Kujawska M, Ignatowicz E, Ewertowska M, Adamska T, Markowski J, Jodynys-Liebert J: Attenuation of KBrO₃-induced renal and hepatic toxicity by cloudy apple juice in rat. *Phytother Res* 2013, 27(8):1214-1219.

23. Ahmad MK, Khan AA, Ali SN, Mahmood R: Chemoprotective effect of taurine on potassium bromate-induced DNA damage, DNA-protein cross linking and oxidative stress in rat intestine. *PloS One* 2015, 10(3):e0119137.
24. Mohamed EA, saddek EA: The protective effect of taurine and/or vanillin against renal, testicular, and hematological alterations induced by potassium bromate toxicity in rats. *The Journal of Basic and Applied Zoology* 2019, 80(3).
25. Sabiu S, Wudil AM, Sunmonu TO: Combined Administration of *Telfairia occidentalis* and *Vernonia amygdalina* Leaf Powders Ameliorates Garlic-induced Hepatotoxicity in Wistar Rats. *Pharmacologia* 2014, 5(5):191-198.
26. Gao F, Horie T: A synthetic analog of prostaglandin E(1) prevents the production of reactive oxygen species in the intestinal mucosa of methotrexate-treated rats. *Life Sci* 2002, 71(9):1091-1099.
27. Parsons JL, Chipman JK: The role of glutathione in DNA damage by potassium bromate *in vitro*. *Mutagenesis* 2000, 15(4):311-316.
28. Naif GA, Jamaan A, Ahmed AA, Saleh NM, Mostafa AA: Deleterious effects of potassium bromate administration on renal and hepatic tissues of Swiss mice. *Saudi Journal of Biological Sciences* 2018, 25(2):278-284.
29. Circu ML, Aw TY: Redox biology of the intestine. *Free Radic Res* 2011, 45(11-12):1245-1266.
30. Akanji MA, Nafiu MO, Yakubu MT: Enzyme activities and histopathology of selected tissues in rats treated with potassium bromate. *African Journal of Biomedical Research* 2008, 11(1):87-95.
31. Dimkpa U, Ukoha UU, Udemezue OO, Okafor JI, Ufondu OA, Anyiam DC: Histopathologic effect of potassium bromate on the kidney of adult Wistar rats. *Tropical Journal of Medical Research* 2012, 16(1):20-23.
32. Valerio DA, Georgetti SR, Magro DA, Casagrande R, Cunha TM, Vicentini FT, Vieira SM, Fonseca MJ, Ferreira SH, Cunha FQ *et al*: Quercetin reduces inflammatory pain: inhibition of oxidative stress and cytokine production. *J Nat Prod* 2009, 72(11):1975-1979.
33. Kaya FF, Topaktas M: Genotoxic effects of potassium bromate on human peripheral lymphocytes *in vitro*. *Mutat Res* 2007, 626(1-2):48-52.
34. Moubarak HS, Essawy TA, Mohammed SS: Carcinogenic effect of potassium bromate on tongue of adult male albino rats. *Journal of Radiation Research and Applied Sciences* 2020, 13(1):121-131.
35. Steven A, Lowe J: *Pathology. In.*, 2nd edn. London, New York: Mosby; 2000: 26.
36. Elbakary NA, Soliman GM, Tawfik SM, Zaher SM: Evaluation of the possible protective role of vitamin A on methotrexate-induced changes on the jejunal mucosa of adult male albino rat: Histological and immunohistochemical study. *Journal of Microscopy and Ultrastructure* 2014, 2(2):77-93.
37. Kumar V, Abbas AK, J.C. A: *Robbins basic pathology. In.*, 9thCanada, Saunders Elsevier edn. Canada Saunders: Elsevier; 2012: 13-14.
38. Jahovic N, Sener G, Cevik H, Ersoy Y, Arbak S, Yegen BC: Amelioration of methotrexate-induced enteritis by melatonin in rats. *Cell Biochem Funct* 2004, 22(3):169-178.
39. Levison DA, Reid R, Burt AD, Harrison DJ, Fleming S: *Muir's Textbook of Pathology*, 14th edn. London, United Kingdom: Taylor & Francis Ltd; 2008.
40. Rubin R, Strayer DS: *Rubin's Pathology. In: Clinicopathologic foundations of Medicine*. 6th edn. Philadelphia, Baltimore: Lippincott Williams & Wilkins; 2012: 14-15.
41. Bayramoglu G, Bayramoglu A, Altuner Y, Uyanoglu M, Colak S: The effects of lycopene on hepatic ischemia/reperfusion injury in rats. *Cytotechnology* 2015, 67(3):487-491.
42. Kim H: Inhibitory mechanism of lycopene on cytokine expression in experimental pancreatitis. *Ann NY Acad Sci* 2011, 1229(1):99-102.
43. Jain D, Katti N: Combination treatment of lycopene and hesperidin protect experimentally induced ulcer in laboratory rats. *J Intercult Ethnopharmacol* 2015, 4(2):143-146.

الملخص العربي

يقلل الليكوبين من التغيرات الهيكلية التي يسببها برومات البوتاسيوم في الغشاء المخاطي الصائم في الجرذان البالغة

نهى جمال بهى ونهى رمضان محمد السويدي
قسم الهستولوجيا وبيولوجيا الخلية - كلية الطب- جامعة طنطا

المقدمة: برومات البوتاسيوم ($KBrO_3$) هو عامل مؤكسد يستخدم على نطاق واسع كمحسن دقيق. ومع ذلك ، فإن له آثارًا سامة على الجينات وكذلك يعتبر عامل مسرطن على أعضاء الجسم المختلفة بطريقة تعتمد على الجرعة ومدة العلاج.

الهدف من هذه الدراسة: استكشاف تأثير برومات البوتاسيوم ($KBrO_3$) على بنية الغشاء المخاطي الصائم للجرذ والتحقيق من الدور المحتمل للليكوبين كجزء مضاف للأوكسدة قوى ، في منع أو تخفيف تأثير برومات البوتاسيوم. **مواد وطرق البحث:** تم استخدام أربعة وعشرين من ذكور الجرذان البيضاء في الدراسة وتم تقسيمها بالتساوي إلى أربع مجموعات تجريبية. المجموعة الضابطة ، مجموعة اللايكوبين التي تلقت 10 ملجم من اللايكوبين / كجم / يوم / عن طريق الفم ؛ مجموعة برومات البوتاسيوم التي تلقت 100 ملجم من برومات البوتاسيوم / كجم / يوم / عن طريق الفم ومجموعة برومات البوتاسيوم والليكوبين التي تلقت برومات البوتاسيوم و الليكوبين بنفس الجرعات كما في المجموعات المستخدمة سابقا. و بعد 4 أسابيع تم تجهيز عينات الغشاء المخاطي الصائم للدراسة الهستولوجية والهستوكيميائية المناعية وكذلك دراسة التركيب الدقيق.

النتائج: أظهر الغشاء المخاطي الصائم للمجموعة المعالجة ببرومات البوتاسيوم زغابات قصيرة وواسعة ، وانقطاع وتقرح لخلاياها الظهارية المبطنة ، وتسلسل خلوي التهابي ، وتوسع في الأوعية الدموية. علاوة على ذلك ، كان هناك انخفاض كبير في عدد الخلايا الكأسية والنواة الاجابية ل PCNA في الصائم.

كما أظهر الفحص الدقيق وجود فجوات في الميتوكوندريا المنتفخة ، وتوسع الشبكة الإندوبلازمية الخشنة مع تقلص النوى الداكنة. ومن المثير للاهتمام ، أن المجموعة التي عولجت بكلا من اللايكوبين و برومات البوتاسيوم أظهرت وجود عدد قليل من الفجوات الحشوية وتشوهات في الميتوكوندريا في الخلايا الظهارية المبطنة للزغب. علاوة على ذلك ، كان هناك تحسن كبير في ارتفاع الزغابات الصائمية ، وعدد الخلايا الكأسية ، وكذلك النواه اجابية PCNA. **الاستنتاج:** يسبب برومات البوتاسيوم تلفًا خلويًا في الغشاء المخاطي الصائم للجرذان والذي تم منعه عن طريق تناول المتزامن للليكوبين.